



AGE OF SEDIMENTS ON DANUBE TERRACES OF THE PEST PLAIN (HUNGARY) BASED ON OPTICALLY STIMULATED LUMINESCENCE DATING OF QUARTZ AND FELDSPAR

EDIT THAMÓ-BOZSÓ¹, GÁBOR CSILLAG^{2,3}, JUDIT FÜRI¹, ATTILA NAGY⁴, ÁRPÁD MAGYARI⁵

¹Mining and Geological Survey of Hungary, Stefánia út 14, 1143 Budapest, Hungary

²Hungarian Academy of Sciences (MTA), Research Centre for Astronomy and Earth Sciences, Institute for Geological and Geochemical Research, Budaörsi út 45, 1112 Budapest, Hungary

³Hungarian Academy of Sciences (MTA) – Eötvös Loránd University (ELTE) Geological, Geophysical and Space Science Research Group, Pázmány Péter sétány 1/c, 1117 Budapest, Hungary

⁴Anteusz Bt., Harminckettesek tere 6, 1086 Budapest, Hungary

⁵MOL Nyrt., Október huszonharmadika u. 18, 1117 Budapest, Hungary

Received 15 September 2019

Accepted 28 August 2020

Abstract

The numerical ages available for the sediments on the Danube terraces in the Pest Plain are scarce. In this study, we present quartz OSL and K feldspar post-IR IRSL₂₉₀ ages for the sandy fluvial, aeolian and slope sediments collected from Danube terraces IIb, III and V.

The feldspar post-IR IRSL₂₉₀ ages without residual dose subtraction are older than the quartz OSL ages, except for one sample, but the two sets of ages are overlapping within one or two sigma errors.

In the bleaching experiment under natural sunlight during summer, an unbleachable component ranging from 2.5±0.7 Gy to 5.2±0.3 Gy after 30 h exposure to bright sunshine is observed and it corresponds to 3–8% of the measured K feldspar post-IR IRSL₂₉₀ equivalent doses. These facts indicate that residual dose subtraction would be necessary before age calculation, in most cases.

The saturated fluvial gravelly sand of terrace V of the Danube is older than ~ 296 ka based on feldspar post-IR IRSL₂₉₀ measurements. This age does not contradict the traditional terrace chronology and the earlier published age data of this terrace. The other studied sediments on the surface of the terraces V, III and IIb deposited much later than the formation of these terraces. They infer aeolian activity and fluvial sedimentation of small streams during the MIS 3 and MIS 2 periods. The age of the dated dune sands with coeval aeolian sediments in Hungary indicate the cold and dry periods with strong wind activity of the Late Weichselian.

Keywords

bleaching experiment, Danube terraces, K-feldspar post-IR IRSL₂₉₀, Late Pleistocene, quartz SAR-OSL, residual dose.

1. Introduction

The Danube terrace staircases in Hungary developed between the uplifting areas of the Transdanubian Range and the North Hungarian Mountains and the subsiding Little Plain and Great Hungarian Plain. Different uplift and subsidence rates and periodic climate changes affected the formation of the terraces during the Late Pliocene and

Pleistocene. The chronology and correlation of the Danube terrace system in Hungary are based on the geomorphic position of the terrace segments, rare palaeontological findings (e.g. Pécsi, 1959; Kretzoi and Pécsi, 1982; Virág and Gasparik, 2012), U/Th ages (e.g. Kele 2009; Sierralta *et al.* 2010), magnetostratigraphy (e.g. Lantos, 2004) and, from recently, cosmogenic nuclide (³He, ¹⁰Be, ²⁶Al) dating and optically stimulated luminescence dating (e.g. Ruzsáczay-

Corresponding author: Mining and Geological Survey of Hungary
e-mail: bozso.edit@mbfsz.gov.hu

Rüdiger *et al.*, 2005b, 2016, 2018). The age of the Pleistocene formations was frequently expressed according to the Alpine chronostratigraphic terminology. Besides this, the recently used Central European chronostratigraphy and/or the marine isotope stages (MIS) are also indicated in this study, according to the Stratigraphic Table of Germany (STD 2016).

Sedimentological and petrological data also support the correlation of the terraces, e.g. roundness of gravels (Pécsiné Donáth 1958; Burján 2000) and heavy minerals (Burján 2003). In the NE part of the Transdanubian Range, at the Gerecse Hills, a new terrace system was established by Csillag *et al.* (2018) and Ruzsiczay-Rüdiger *et al.* (2018) with new chronology on the basis of the novel age data together with the geomorphological, geological and palaeontological observations. But numerical age data and palaeontological findings are very scarce in the Pest Plain. Therefore, the first aim of this study was to date sediments on the area of the Danube terraces on the Pest Plain. The second aim was to compare the optically stimulated luminescence ages of coarse-grain quartz and feldspar of the same sediments. Hence, sandy sediments were collected from five outcrops and dated by SAR-OSL and post-IR IRSL₂₉₀ methods.

2. Geology and Geomorphology of the Study Area

The study area is the Pest Plain (Figs. 1 and 2). It is situated near River Danube in the surroundings of Budapest, between hilly areas (Gödöllő Hills, Buda Mountains and Visegrád Mountains). The basement of this plain lies about 600–1500 m in depth, and consists of Upper Triassic and Lower Jurassic dolomite and limestone, which was formed from the sediments of the Tethys sea (Haas *et al.*, 2010). These Mesozoic carbonate rocks are covered by Eocene limestone and marl. Above them, hundreds meter thick sediments of the Paratethys sea were deposited, mainly Oligocene and Miocene clay, sandstone, sand and limestone, with intercalations of thin volcanic tuff layers (Jámbor *et al.*, 1966b). In the Late Miocene, after the folding and uplifting of the Carpathians due to the subduction of the European foreland (Horváth, 1993), the area was part of the brackish–freshwater Lake Pannon, which as a remnant of the Paratethys sea occupied the Pannonian Basin. The lake was filled with the sediments of fluvial-dominated delta systems prograding from NW and NE directions (e.g. Magyar *et al.*, 2013). The deltas gradually transformed into alluvial plains and the Hungarian part of the lake was

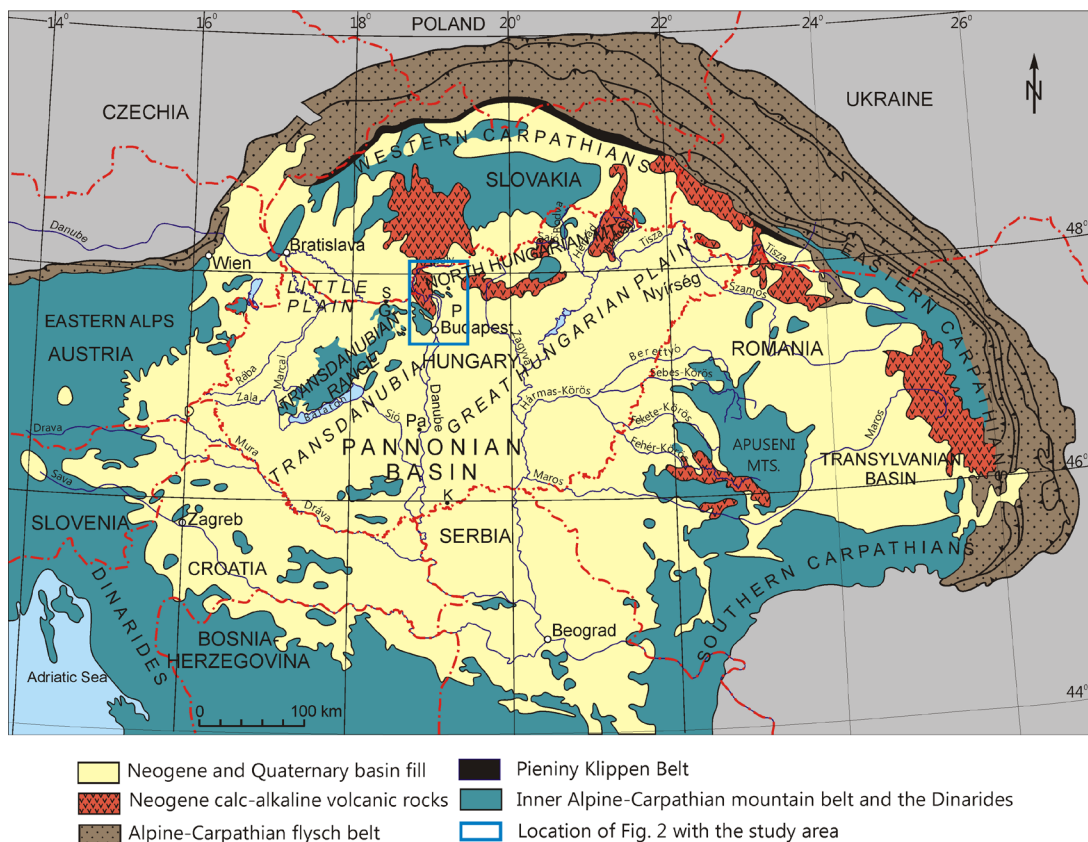


Fig 1. Location of the study area and geological surroundings after Horváth and Cloething (1996). P: Pest Plain, G: Gerecse Hills, S: Süttő, K: Katymár, Pa:Paks.

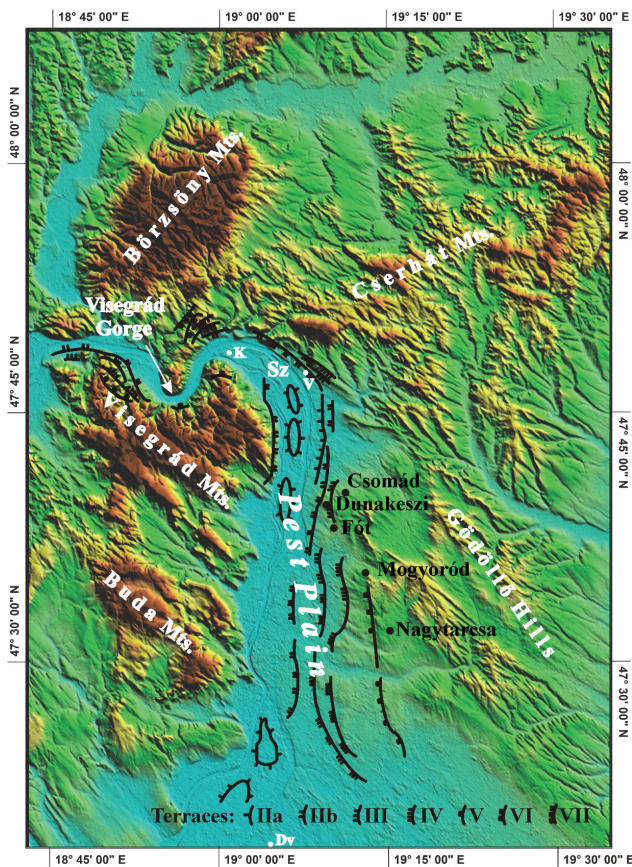


Fig 2. Pest Plain and the surrounding areas with the locations of the sampling sites and the terraces of the Danube. Terraces are based on Pécsi *et al.* (2000), Sz: Szentendre Island, K: Kisoroszi, V: Vác, Dv: Dunavarsány.

filled up by the Pliocene (e.g. Gábris and Nádor, 2007). From the Late Miocene, certain areas were subsided and others were uplifted due to the NW–SE and N–S compression stress field (e.g. Horváth and Cloetingh, 1996; Fodor *et al.*, 2005). The course of the rivers was influenced largely by the neotectonic deformations. In the Late Pliocene, the Palaeo-Danube probably flowed in the western part of Transdanubia, far from the recent channel of the Danube (Szádeczky-Kardoss, 1938, 1941; Gábris and Nádor, 2007). There is no consensus on the date, when the Palaeo-Danube changed its flow direction and cut the Miocene andesites of the Visegrád and Börzsöny Mountains at the Visegrád Gorge (Fig. 2). Urbancsek (1960) and Borsy (1989) supposed that it happened during the Late Pliocene; Mike (1991) and Neppel *et al.* (1999) presumed the Günz–Mindel (Cromer–Elster) interglacial. However, based on the palaeontological and paleomagnetic data (Kretzoi and Pécsi, 1982; Lathman and Schwarcz, 1990) the maximum age of this incision is Early Pleistocene (2.4–1.4 Ma). But, assuredly, after the Palaeo-Danube cut the Visegrád Gorge, it flowed in the SE direction for a long time, and not in

its recent N–S course, collecting the water and sediments of many palaeo rivers (Gábris 1998, 2002). Then, due to neotectonic movements, the channel of the Palaeo-Danube gradually shifted from east to west, and the river reached its recent N–S flow direction during the Riss–Würm interglacial (Urbancsek 1960) which corresponds to MIS 5e or Eemian interglacial period, or only in the Holocene (Somogyi, 1961; Rónai, 1985).

On the uplifting areas northwest from the Pest Plain, six or maximum eight terraces were developed at the Danube band, according to Pécsi (1959) and Kretzoi & Pécsi (1982), and in the Gerecse Hills, eleven terraces were recently identified by Csillag *et al.* (2018). On the Pest Plain, between the uplifting hilly areas, five Pleistocene terraces were formed by the Danube, based on the traditional terrace classification (Fig. 3; Pécsi, 1958, 1959).

The valley of the Danube is located at about 122 m asl. in the northern part of the Pest Plain and at 97 m asl. in the southern part of it, at Budapest. Towards south, the terraces lie gradually at lower altitude in the direction of the sinking Great Hungarian Plain, where the river built a huge alluvial fan.

First of all, the position and characteristics of the terraces on the Pest Plain were studied in detail by Pécsi (1958, 1959, 1996). According to him, terraces V and IV occur only in the south-eastern part of the Pest Plain. Terrace V is built up from gravel with about 14 m thickness, while terrace IV consists of a 1–2 m thick gravel layer with 3–4 m sand on it. The sediments show signs of cryoturbation and solifluction. The gravels are mainly from quartz

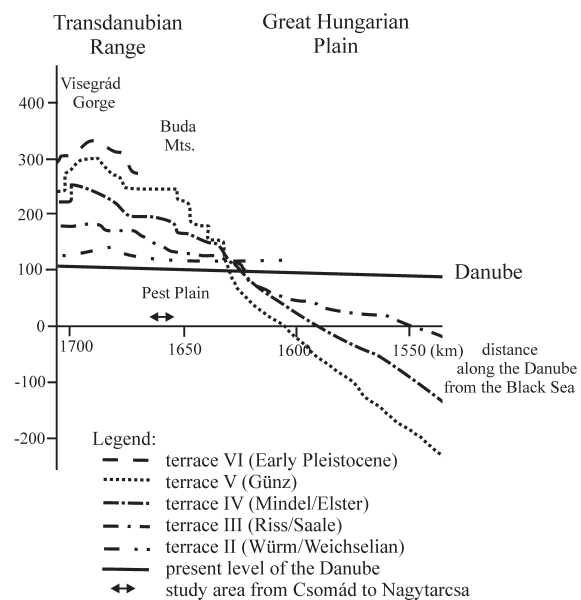


Fig 3. Traditional terrace system on the Pest Plain and in the surrounding areas after Pécsi (1959).

and quartzite, and partly from andesite of the Visegrád Mountains, and limestone from the Gerecse Hills of the Transdanubian Range. In some places, these sediments are covered by travertine. Based on fossils of *Mastodon borsoni* (*Mammot borsoni*), it was thought that terrace V was developed during the Günz (~Cromer), but the last occurrence of the *Mammot borsoni* is much older, 2.0–2.4 Ma according to Virág (2013). *Mastodon* (*Dibunodon*) *arvernensis*, *Mammuth americanus praetypicus* and *Dicerorhinus megarhinus* remnants were also found in this gravel body (Jámbor *et al.* 1966a) and bones of Late-Pliocene *Stephanorhinus megarhinus* were described at Rákos, in the eastern part of Budapest (Kretzoi 1981). The cosmogenic ^3He exposure minimum age of terrace V is 800 ka (Ruszkiczay-Rüdiger *et al.* 2005a). Remnants of *Elephas trogontherii* (*Mammuthus trogontherii*) in terrace IV were counted to the Mindel glaciation (Pécsi, 1959) which correspond to Elster glaciation or MIS 10, but the age of these fossils is from 0.8–0.7 Ma to ~0.2 Ma (Virág, 2013). The incision of this terrace happened between 410 and 390 ka ago (in MIS 11) due to a sudden warming episode, according to the termination model (Gábris, 2006, 2013).

Terrace III runs in a narrow range between the older and younger terraces, 27–30 m above the recent level of the Danube. Its age is Riss (Saale, MIS 8 – MIS 6) according to Pécsi (1959), or minimum 170 ka (Ruszkiczay-Rüdiger *et al.*, 2005a). This terrace can be divided into IIIb and IIIa terraces, and their staircases were formed by the incision of the Danube 330–315 ka and 220–190 ka ago, respectively (Gábris, 2006, 2013). In some places, the fluvial sediments of this terrace are covered by 190–175 ka old travertine (Scheuer & Schweitzer, 1988).

Terrace II also consists of two levels. Terrace IIb can be followed through the Pest Plain parallel to the Danube. The gravel layer of this terrace is about 7–10 m thick and lies at about 15–20 m above the current level of the Danube. The quartz and quartzite gravels of the younger terrace sediments are more rounded (Pécsiné Donáth 1958). *Elephas primigenius* (*Mammuthus primigenius*) bones at Vác and Budapest indicate Late Riss (Late Saale) and Early Würm (Early Weichselian) (Pécsi, 1959). According to Gábris (2006, 2013), the stair of terrace IIb was formed by incision between 130 and 123 ka. 2–3 m thick fluvial sand and several meters thick aeolian sand cover the gravel. They show solifluction phenomena at some places. Loess with 1–2 palaeosol layers also can be found on this terrace.

Terrace IIa is 8–10 m above the current level of the Danube and developed at the end of the Pleistocene, during the Late Würm (Late Weichselian) period. The stair of this terrace started to form after the Last Glacial Maximum, or about 19–17 ka ago (Gábris, 2006, 2013). Usually, this terrace is covered by aeolian sand. 18 ± 2.5 ka old fluvial sediments and 16–0.6 ka old aeolian sands with paleosoils

between them were dated by luminescence (TL, IRSL) and radiocarbon methods at Kisoroszi and Dunavarsány (Fig. 2, Ujházi *et al.*, 2003; Gábris, 2003).

Terrace I is represented by overbank sediments at 5–7 m above the current level of the Danube. It is built up of fluvial sand and silt, which were deposited during the Early Holocene. The lowest level along the river also consists of overbank deposits, but in the lower position, 0–5 m above the level of Danube (Pécsi, 1996). In the abandoned arms of the Danube swampy environments developed.

The terrace levels are not in their original position because the neotectonic movements replaced them into gradually lower positions in the direction of the sinking Great Hungarian Plain (Fig. 3).

The surface of the terraces was altered during the forthcoming interglacial and glacial periods. They were covered mainly by aeolian sediments (loess or aeolian sand), and in some places by fluvial sediments and travertine. Under the modern soil layer mostly Weichselian sediments can be found. During the cold and dry periods in the Weichselian open coniferous taiga forests and steppe mosaics were characteristic for the plain areas of Hungary (Járainé Komlódi, 2000). This climate and the scarce vegetation favoured the sand and silt movement by strong winds, first of all, during the Weichselian High Glacial in MIS 3, and the Last Glacial Maximum in MIS 2. Loess formation in MIS 3 and MIS 2 was documented in many places of Hungary (e.g. Sümegi and Krolopp, 1995; Novothny *et al.*, 2010b, 2011; 2020; Gábris *et al.*, 2012; Thiel *et al.*, 2014). Aeolian sand bodies, which were dated on the terraces and alluvial fans deposited mainly in MIS 2 according to the above-mentioned references and also e.g. Novothny *et al.* (2010a), and in MIS 3 as well (Sümegi *et al.*, 2019). During milder or warmer phases, forest-steppe and pine-birch forests mixed with deciduous trees expanded (Járainé Komlódi, 2000), and mainly chernozem or chernozem-like and forest paleosoils developed on the loess and blown sand (e.g. Gábris *et al.*, 2012).

3. Samples and Study Methods

3.1 Samples

For optically stimulated luminescence dating, the samples were collected by opaque PVC tubes from five outcrops on different terraces of the Danube (Table 1; Fig. 2). For environmental dose determination, about 1 kg bulk samples were collected from the near surroundings of each OSL samples. In addition, some sediment was taken into tight closed containers (plastic boxes) for water content measurements.

Two fluvial samples, medium-grained sand with gravel are from the Nagytarcsa gravel mine which represents terrace V according to the geomorphological map of Pécsi *et al.* (2000). The samples are from a depth of 7.0 and 7.9 m under the current surface (Fig. 4E). The 10–12 m thick ter-

Table 1. Location and main characteristics of the samples.

Location	Terrace level	Latitude (N)	Longitude (E)	Altitude (m asL)	Sample	Nr.	Depth (cm)	Sediment	Facies
Nagytarcsa gravel mine	V	47.52822	19.25767	170.52	Nt1	120.1.	700	medium sand with gravel	fluvial
					Nt2	120.2.	790	medium sand with gravel	fluvial
Mogyoród gravel mine	V	47.58594	19.22269	247.66	Mgy1	119.1.	130	fine sand	dune
					Mgy2	119.2.	240	fine sand	dune
Csomád sand mine E wall	III	47.67194	19.18694	146.49	Csm1	122.1.	160	silty fine sand	dune
					Csm2	122.2.	320	silty fine sand	dune
Csomád sand mine W wall	III	47.67131	19.18592	150.81	Csm3	122.3.	240	fine-medium sand	fluvial
					Csm4	122.4.	440	fine-medium sand	fluvial?
Fót sand mine	III	47.64511	19.17714	175	Ft1	123.1.	180	fine-medium sand	slope, reworked fluvial
					Ft2	123.2.	350	fine-medium sand	slope, reworked fluvial
					Dk1	121.1.	190	medium sand	dune
					Dk2	121.2.	360	medium sand	dune
					Dk3	121.3.	410	medium sand	fluvial
Dunakeszi sand mine	IIb	47.66083	19.15706	165.47	Dk4	121.4.	590	fine sand	fluvial
					Dk5	121.5.	740	fine-medium sand	fluvial

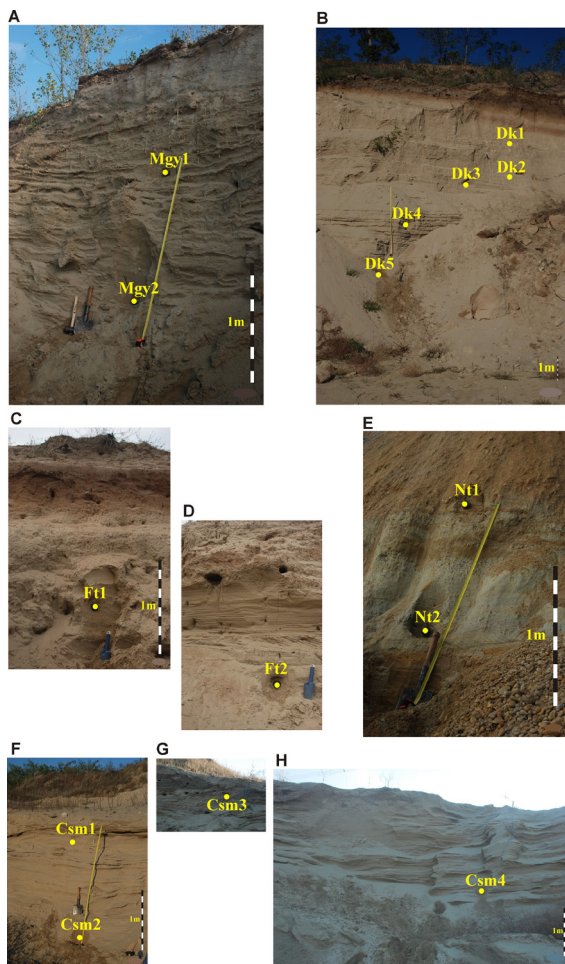


Fig 4. Position of the samples in the sampling sites. A: Mogyoród gravel mine (aeolian sand), B: Dunakeszi sand mine (fluvial and aeolian sand), C-D: Fót sand mine (slope, reworked fluvial sand), E: Nagytarcsa gravel mine (fluvial sand), F: Csomád sand mine East wall (aeolian sand), G-H: Csomád sand mine West wall (fluvial sand).

race sediments consist of gravel and gravelly sand layers with planar and cross lamination. The average size of the gravels is 2–6 cm. Quartzite and weathered volcanic rock gravels are abundant, while chert gravels are rare. The volcanic rock gravels originated from the Visegrád Mountains (Fig. 2).

Aeolian fine sand layers at 1.3 and 2.4 m depth were sampled from a dune on terrace V in the Mogyoród gravel mine (Fig. 4A). The ~3.5 m high dune is built up from fine and medium grained sand layers with cross stratification. Under the dune the gravel layer of the terrace is only 0.5–0.6 m thick, and contains mainly quartzite, weathered volcanic rock and subordinately gneiss gravels.

Four samples were collected for dating from the Csomád sand mine on terrace level III (Fig. 4F-H). Two aeolian silty fine sand samples are from the East wall of the mine at depth 1.6 and 3.2 m. The other two samples are fluvial fine-medium grained sands from the West wall of the mine from 2.4 and 4.4 m depth, which represent the sediments of a small stream. The sand bodies are cross-laminated and their thickness in the outcrops is about 2 and 3 m, respectively.

Reworked fluvial fine-medium sands of slope sediments were sampled for dating on terrace III in the Fót sand mine, from a depth of 1.8 and 3.5 m (Fig. 4C and D). The total thickness of these sediments is about 3 m and they show cross and planar lamination.

On terrace IIb, fluvial and aeolian fine and medium-grained sand samples were studied between depths of 1.9 and 7.4 m in the Dunakeszi sand mine (Fig. 4B). Here the minimum 2.5 m thick fluvial sand of a stream shows mainly planar bedding and contains thin gravel layers and lenses. Quartz, quartzite and relatively fresh volcanic rocks are frequent with a size of 0.3–1.0 cm. The thickness of

the aeolian sand is about 2–3 m. It is cross-laminated and contains many rhizoconcretions.

3.2 Sample preparation

Sample preparation for optically stimulated luminescence dating was carried out under subdued red light conditions. Quartz and K-feldspar grains were extracted from the 0.1–0.2 mm grain size fraction of the sediments using 20% H₂O₂ to remove the organic material, 10% HCl to dissolve carbonates, 0.01N Na₂C₂O₄ for desaggregation and cleaning of the surface from the grains, and aqueous solution of sodium polytungstate (3Na₂WO₄ · 9WO₃ · H₂O, SPT) with 2.67 and 2.58 g/cm³ for density separation. After these treatments, the quartz separates were etched by 40% HF for 90 min, or samples Dk1-5 for 60 min, to eliminate the outer 10–15 μm layer from the surface of the grains which was affected by the environmental alpha radiation. Then, 10% HCl was used to dissolve fluorides which were precipitated during etching. Finally, the 0.10–0.16 mm quartz and feldspar grains were separated by dry sieving.

The grains were mounted in monolayer on stainless-steel discs using silicone oil spray. The size of the aliquots was 2 mm diameter (small aliquot) in the case of feldspar, and 5 mm diameter (medium aliquots) in the case of quartz due to the relatively weak OSL signal of the quartz of the studied samples.

Before gamma spectrometry measurements, the bulk samples were dried, and the >1 mm grains were crashed. The sediments were filled into Marinelli beakers and they were stored in the closed containers for more than 28 days to reach equilibrium between radon and its daughter isotopes.

3.3 Optically stimulated luminescence measurements

Luminescence measurements were made by Risø TL/OSL DA-15C/D and DA-20 readers in 2013 and 2019. Blue light stimulated luminescence of quartz was detected through a Hoya-340 filter, while infrared light stimulated luminescence of feldspar through a Schott BG-39 and Corning 7-59 filter combination. A calibrated 90Sr/90Y beta source was used for irradiation with a dose rate of about 0.092 Gy/s in 2013, and 0.081 Gy/s in 2019.

Single-Aliquot Regenerative-dose (SAR) OSL protocol (Wintley and Murray, 2006) was used on quartz, and post-IR IRSL (290 °C) on feldspar (Thiel *et al.*, 2011, 2012). In the case of quartz, according to the results of the preheat plateau test, 240°C preheat temperature was applied during the OSL measurements of the samples from the Dunakeszi sand mine, while 260°C preheat temperature for the other samples, and the cut heat was 200°C. The thermal transfer test indicated that the thermal transfer is negligible using these preheat temperatures. The purity of the quartz separates was checked by the measurement of OSL depletion

due to infrared stimulation on every measured aliquot in an additional last cycle of the SAR-OSL protocol. During the evaluation of the OSL signals, early-background subtraction method (Cunningham and Wallinga, 2010) was applied, *i.e.*, the 0.8–1.6 s integral of the OSL decay curve was subtracted from the initial 0.8 s integral signal to avoid a contribution from medium and slow components. The dose-response curves were fitted by single saturation exponential function. The dose recovery test was performed on 3 aliquots of each sample which display natural luminescence signals below saturation level.

K-feldspar was measured by post-IR IRSL₂₉₀ protocol with 320°C preheat before IR stimulation at 50°C for 200 s, then at 290°C for 200 s, and illumination at 325°C for 100 s in the last step of each cycle according to Thiel *et al.* (2011; 2012). The test doses were relatively small, about 15% of the natural equivalent doses. From the initial 2 s of the post-IR IRSL₂₉₀ signal the last 40 s was subtracted, similarly to Thiel *et al.* (2012). A single saturation exponential function was used for fitting dose-response curves.

Residual doses and dose recovery ratios of the feldspar separates were measured after 12 h bleaching on changeable (sometimes cloudy) sunlight in winter except for the saturated samples. The bleachability of the post-IR IRSL₂₉₀ signal of four feldspar separates was also observed by bleaching them on bright sunlight in summer (in August) for 4, 8, 12, 16, 20, 26 and 30 h before the residual dose determination. The fading test according to Auclair *et al.* (2003) was performed with 26.3 h maximum delay time on one aliquot of each K-feldspar separate, which natural luminescence signal lies below saturation level. The given dose was close to the natural equivalent dose of the samples.

3.4 Dose rate determination

Calculation of the environmental dose rates is based on laboratory high-resolution gamma spectrometry measurements. They were made by Canberra GC3020 on 0.8–1.0 kg bulk samples, and provide U, Th and K concentrations. Dose rate conversion factors given by Adamiec and Aitken (1998), attenuation factors of Mejdahl (1979) were applied. 12.5±0.5% K concentration (Huntley and Baril, 1997) and 0.15±0.05 a-value (Balescu and Lamothe, 1994) were used during the calculation of the internal dose rate of feldspar. The cosmic dose rate was determined according to Prescott and Stephan (1982) and Prescott and Hutton (1994).

The water content of the sediments was determined at the time of sampling and after saturation by water in a laboratory. The results helped to estimate the water content of the dated sediments during the time period of burial. It was taken 5±1% for the dune sands, and 11±2%, 14±3% or 18±3% for the fluvial sediments (Table 2).

Sample preparation, luminescence, gamma spectrometry, and water content measurements were carried out at

Table 2. Dose rate determination.

Sample	Depth (cm)	U (ppm)	Th (ppm)	K (%)	Water content (dryw%)	Dose rate (Gy/ka)	
						Quartz	K-feldspar
Nt1	700	0.81 ± 0.02	2.49 ± 0.04	1.02 ± 0.01	18 ± 3	1.22 ± 0.09	1.85 ± 0.19
Nt2	790	0.75 ± 0.02	2.74 ± 0.03	1.04 ± 0.01	18 ± 3	1.23 ± 0.09	1.86 ± 0.19
Mgy1	130	1.72 ± 0.02	6.06 ± 0.05	0.79 ± 0.04	5 ± 1	1.69 ± 0.12	2.44 ± 0.17
Mgy2	240	2.00 ± 0.04	7.25 ± 0.06	0.83 ± 0.03	5 ± 1	1.85 ± 0.13	2.63 ± 0.19
Csm1	160	1.45 ± 0.02	4.15 ± 0.05	1.18 ± 0.04	5 ± 1	1.87 ± 0.13	2.57 ± 0.19
Csm2	320	2.17 ± 0.05	7.20 ± 0.06	1.12 ± 0.05	5 ± 1	2.14 ± 0.16	2.93 ± 0.21
Csm3	240	1.59 ± 0.02	5.01 ± 0.04	0.91 ± 0.04	14 ± 3	1.54 ± 0.11	2.25 ± 0.16
Csm4	440	1.53 ± 0.03	4.82 ± 0.04	0.90 ± 0.03	14 ± 3	1.48 ± 0.10	2.18 ± 0.15
Ft1	180	1.95 ± 0.05	3.81 ± 0.04	0.80 ± 0.02	11 ± 2	1.50 ± 0.10	2.22 ± 0.15
Ft2	350	1.95 ± 0.06	3.17 ± 0.03	0.83 ± 0.03	11 ± 2	1.46 ± 0.10	2.16 ± 0.15
Dk1	190	0.78 ± 0.01	1.95 ± 0.03	0.82 ± 0.03	5 ± 1	1.24 ± 0.09	1.86 ± 0.13
Dk2	360	1.22 ± 0.02	3.85 ± 0.04	0.81 ± 0.03	5 ± 1	1.42 ± 0.10	2.10 ± 0.15
Dk3	410	1.19 ± 0.03	3.10 ± 0.03	0.81 ± 0.03	11 ± 2	1.28 ± 0.09	1.93 ± 0.14
Dk4	590	1.42 ± 0.02	3.79 ± 0.04	0.89 ± 0.04	11 ± 2	1.41 ± 0.10	2.09 ± 0.15
Dk5	740	1.34 ± 0.03	4.18 ± 0.04	0.87 ± 0.04	11 ± 2	1.39 ± 0.10	2.07 ± 0.15

the Mining and Geological Survey of Hungary (MBFSZ, former Geological and Geophysical Institute of Hungary).

4. Results and Discussion

The results of dose rate determination are in Table 2. The optically stimulated luminescence test measurements indicated that quartz and K-feldspar fractions of the samples are good for precise age dating, except two samples with saturated quartz OSL and feldspar post-IR IRSL₂₉₀ signals.

4.1 OSL measurements on quartz

Dose recovery ratios of quartz are satisfactory, 1.05 ± 0.02 on average ($n=39$, Table 3). Some aliquots were rejected due to an inadequate result of IR test (feldspar or mica contamination), or high recuperation, or bad recycling ratio. Recuperation of the accepted aliquots is low, 1.02 ± 1.09 on average ($n=403$). Quartz OSL dating is based on equivalent doses of 23–56 aliquots per sample (Table 4). The D_e values of the studied quartz fractions have a relative error in a range of 3.9–9.6%, precision (reciprocal standard error) ~ 10 –25, and relatively high dispersion. These characteristics were visualised in the bivariate plots (radial plots based on Galbraith, 1988; Galbraith and Roberts, 2012) of abanico plots (Dietze *et al.*, 2016). The representative examples are shown in Fig. 5A and C. On the right side of the abanico plots the histograms refer to more or less symmetric D_e dis-

Table 3. Dose recovery ratios.

Sample	Dose recovery ratio	
	Quartz OSL	K-feldspar post-IR IRSL ₂₉₀
Mgy1	1.01 ± 0.10	1.02 ± 0.09
Mgy2	1.03 ± 0.02	1.00 ± 0.10
Csm1	0.98 ± 0.07	1.01 ± 0.08
Csm2	0.96 ± 0.09	1.02 ± 0.05
Csm3	0.99 ± 0.08	1.08 ± 0.05
Csm4	1.01 ± 0.06	1.10 ± 0.04
Ft1	0.99 ± 0.07	1.08 ± 0.01
Ft2	0.97 ± 0.05	1.02 ± 0.07
Dk1	0.99 ± 0.02	0.97 ± 0.11
Dk2	1.03 ± 0.04	0.97 ± 0.15
Dk3	0.98 ± 0.07	0.98 ± 0.13
Dk4	0.98 ± 0.05	0.99 ± 0.09
Dk5	1.02 ± 0.06	0.96 ± 0.14

tributions, and the kernel density estimate curves indicate that the D_e -s of each sample belongs to one population.

In the case of sample Dk4 more than fifty aliquots were measured to get more symmetric distribution. Except for two samples, the overdispersion of the D_e -s changes between 12 and 22% (Table 4; Fig. 5A), indicating that the quartz of these

Table 4. Dating result of quartz and K-feldspar.

Sam- ple	Depth (cm)	Quartz OSL				K-feldspar post-IR [ZSL] ²⁹⁰						K. -feldspar age/Quartz age						
		n	De mean (Gy)	OD (%)	Age (ka)	n	Residual dose (Gy)		Residual dose (%)**		Age (ka)	s. subtr.	no subtr.	w. subtr.	s. subtr.			
							w.	s.	w.	s.						a.	no subtr.	w. subtr.
NT1	700				3	546*												
NT2	790				3	537*												
Mgy1	130	24	62.9 ± 2.7	18 ± 3	37.1 ± 3.1	10	100.3 ± 3.1	9 ± 2	14.6 ± 0.6	14.6	9.5	41.0 ± 2.3	35.0 ± 2.1	1.10 ± 0.11	0.94 ± 0.10			
Mgy2	240	25	70.4 ± 3.7	22 ± 3	38.1 ± 3.3	9	99.7 ± 2.9	7 ± 2	19.2 ± 3.0	19.2	7.4	37.9 ± 1.9	30.6 ± 1.7	0.99 ± 0.10	0.80 ± 0.08	0.92 ± 0.09		
Csm1	160	24	73.3 ± 3.3	20 ± 3	39.3 ± 3.4	10	115.4 ± 3.1	7 ± 2	18.7 ± 4.1	16.2	6.4	44.9 ± 2.3	37.7 ± 2.0	1.14 ± 0.11	0.96 ± 0.10	1.07 ± 0.11		
Csm2	320	23	91.0 ± 3.6	18 ± 3	42.6 ± 3.6	11	126.2 ± 4.8	11 ± 3	16.3 ± 3.9	13.0	1.0	43.1 ± 2.4	37.5 ± 2.2	1.01 ± 0.10	0.88 ± 0.09			
Csm3	240	25	43.9 ± 2.9	29 ± 4	28.5 ± 2.8	9	69.6 ± 1.7	6 ± 2	13.4 ± 3.6	19.2	7.9	30.9 ± 1.8	25.0 ± 1.5	1.09 ± 0.12	0.88 ± 0.10			
Csm4	440	24	45.7 ± 2.3	21 ± 3	30.9 ± 2.6	11	76.5 ± 2.2	8 ± 2	13.3 ± 2.5	17.4	12.0	35.2 ± 2.1	29.0 ± 1.8	1.14 ± 0.12	0.94 ± 0.10			
Ft1	180	27	22.8 ± 0.9	18 ± 3	15.1 ± 1.2	11	35.0 ± 0.9	7 ± 2	7.8 ± 0.2	22.2	10.2	4.3	15.8 ± 0.9	12.3 ± 0.7	1.05 ± 0.10	0.81 ± 0.08	0.94 ± 0.09	
Ft2	350	25	33.3 ± 0.9	12 ± 2	22.8 ± 1.8	11	52.5 ± 1.5	9 ± 2	11.5 ± 3.5	21.9	6.3	24.3 ± 1.4	19.0 ± 1.2	1.07 ± 0.10	0.83 ± 0.08			
Dk1	190	24	16.8 ± 0.7	21 ± 3	13.6 ± 1.2	12	33.2 ± 0.6	5 ± 1	7.4 ± 1.0	22.3	23.9	17.9 ± 1.1	13.9 ± 0.9	1.31 ± 0.14	1.02 ± 0.11			
Dk2	360	25	20.0 ± 1.0	22 ± 4	14.1 ± 1.2	11	35.7 ± 0.5	4 ± 1	10.0 ± 0.9	28.1	10.8	17.1	17.0 ± 0.9	12.2 ± 0.7	1.21 ± 0.12	0.87 ± 0.09	1.08 ± 0.11	
Dk3	410	26	19.4 ± 1.2	30 ± 4	15.2 ± 1.5	11	35.7 ± 0.9	7 ± 2	9.2 ± 0.2	25.9	17.7	18.5 ± 1.1	13.7 ± 0.9	1.22 ± 0.14	0.90 ± 0.10			
Dk4	590	56	21.2 ± 0.7	22 ± 2	15.0 ± 1.2	12	39.3 ± 1.0	7 ± 2	9.0 ± 2.2	22.9	19.9	18.8 ± 1.1	14.5 ± 0.9	1.25 ± 0.13	0.96 ± 0.10			
Dk5	740	29	21.9 ± 0.8	17 ± 3	15.8 ± 1.3	10	39.8 ± 0.7	4 ± 1	10.6 ± 0.3	26.7	17.8	19.2 ± 1.1	14.1 ± 0.8	1.22 ± 0.12	0.89 ± 0.09			

n: number of aliquots; OD: overdispersion; *: 2xDb; **: residual dose in % of the measured natural dose;

w: residual dose after 12 h exposure to changeable sunshine in winter;

s: residual dose after 4 h exposure to bright sunlight in summer;

a: assumable residual based on the correlation with quartz ages;

no subtr.: feldspar age without subtraction of residual dose;

w. subtr.: feldspar age with subtraction of residual dose after 12 h exposure to changeable sunshine in winter;

s. subtr.: feldspar age with subtraction of residual dose after 4 h exposure to bright sunlight in summer.

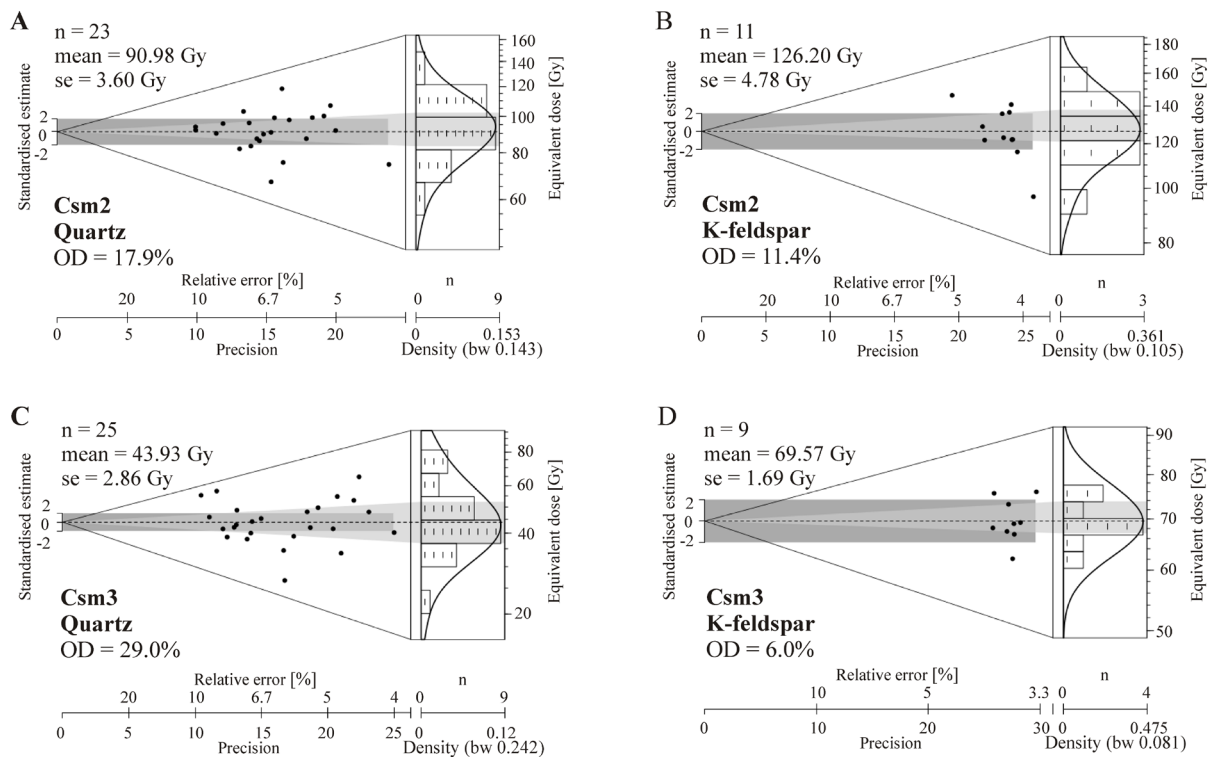


Fig 5. Representative examples for visualisation of the characteristics and distributions of the equivalent doses in abanico plots. A and C: D_e -s were measured by SAR-OSL protocol on medium (5 mm) aliquots of quartz, B and D: D_e -s were determined with post-IR IRSL₂₉₀ protocol on small (2 mm) aliquots of K-feldspar. (Abanico plot: <http://rlum.geographie.uni-koeln.de:9418/packages/RLumShiny/inst/shiny/abanico/>).

sediments was probably well bleached at the time of deposition according to Olley (2004). Therefore, their age was calculated by the mean D_e values, which are almost identical to the central D_e -s, using the central age model of Galbraith *et al.* (1999). But, the equivalent doses of the quartz from fluvial samples Csm3 (Fig. 5C) and Dk3 show 29% and 30% overdispersion values. The large spread of D_e -s (9–32 Gy and 20–80 Gy respectively) can be caused by beta dose heterogeneity, partial or heterogeneous bleaching, and post-depositional disturbance (Olley, 2004). There is no sign of post-depositional disturbance in the studied sections. Probably, the quartz of these samples was not partially bleached before deposition because their kernel density plots in the abanico plots show only one D_e population and their mean and central natural equivalent doses are also very close to each other (central value is 44 ± 3 Gy for Csm3, and 19 ± 1 Gy for Dk3). Therefore, despite the larger overdispersion the quartz age of these two samples was calculated by the mean D_e -s. The quartz OSL ages of the dated sediments range between 14 ± 1 and 43 ± 4 ka (Table 4).

Figure 5 and overdispersion values in Table 4 show that the measured quartz medium aliquots have more heterogeneous dose distribution than in the case of K-feld-

spar small aliquots. As it can be supposed that the dated sediments were well bleached before burial, the more heterogeneous distribution of D_e -s in quartz is probably caused by the heterogeneity in the environmental beta dose rate. This can be the result of the microscopic fluctuations in the spatial distribution of feldspar containing beta emitter ^{40}K (Mayya *et al.*, 2006). In addition, the different amounts of radioactive inclusions in the quartz grains, which lead to a small internal alpha dose rate (Galbraith and Roberts, 2012), cause heterogeneous distribution of internal dose rates.

4.2 Post-IR IRSL₂₉₀ measurements on K-feldspar

Every measured aliquot of K-feldspar showed a good recycling ratio in the range of 1.0 ± 0.1 , and except three rejected aliquots they had recuperation under 5%. Residual doses after 12 h bleaching under changeable sunlight in winter are about 7–19 Gy on average (Table 4), while after the same duration of bleaching under bright sunshine in summer are about 3–5 Gy on average (which correspond to 13–28% and 4–10% of the mean natural equivalent doses respectively). The dose recovery ratios changed between 0.79 and 1.14 (from 0.96 ± 0.14 to

1.1±0.04 on average, Table 3), but, the poor dose recovery ratio of post-IR IRSL₂₉₀ signal of K-feldspar does not necessarily mean an inaccurate measurement of D_e (Buylaert *et al.*, 2012). The fading test of these samples indicates relatively low fading rates or g-values between 0.95 and 1.48%/decade (1.26±0.21%/decade on average). The fading experiments of Thiel *et al.* (2011) indicated that the small fading rate of post-IR IRSL₂₉₀ signal of K-feldspar may be a laboratory artefact. Therefore, fading correction was not applied. Feldspar dating of the non-saturated samples is based on equivalent doses of 9–12 aliquots per sample. Their D_e values show lower relative error (2.5–6%), higher precision (17–40), and lower dispersion than in the case of the quartz fractions of the same samples. The distributions of the equivalent doses are more or less symmetric and their kernel density estimate curves show one D_e population. Two representative examples are presented in the abanico plots of Fig. 5 B and D. The relatively small overdispersion of the D_e values (between 4% and 12% on average, Table 4) probably indicate well-bleached sediments at the time of deposition according to Olley *et al.* (2004). The difference between the mean and the central equivalent doses is a maximum of 1%. Hence, the ages were calculated by the mean D_e values.

Two samples (Nt1 and Nt2) are saturated as their natural post-IR IRSL₂₉₀ signals (Ln/Tn) lie above the saturation level. The minimum age of these samples was calculated with the 2*D₀ values, which correspond to approximately 86% of the dose-response curve (Murray *et al.*, 2014).

In the bleaching experiment in natural sunlight during summer the measured post-IR IRSL₂₉₀ residual doses of the four K-feldspar separates (Mgy2, Csm1, Ft1 and Dk2) ranged from 3.6±0.4 Gy to 7.4±0.5 Gy after 4 h exposure to bright sunshine, then they decreased more slowly with some scatter, and they were between 3.0±0.1 Gy and 5.2±0.6 Gy after 12 h exposure to sunshine, then an unbleachable component ranged from 2.5±0.7 Gy to 5.2±0.3 Gy after 30 h exposure to bright sunshine. The latter corresponds to 3–8% of the measured K-feldspar post-IR IRSL₂₉₀ natural doses. K-feldspar of samples Mgy2 and Csm1 bleached slightly more rapidly than that of samples Dk2 and Ft1 (Fig. 6). Residual doses measured after 12 h exposure to changeable sunshine in winter varied from 7.4±1.0 Gy to 19.2±3.0 Gy and correspond to about 13–28% of the measured K-feldspar post-IR IRSL₂₉₀ natural doses.

Except for one sample (Mgy2), the feldspar ages without residual dose subtraction are older than the quartz ages of the same samples, and the ratio of them range between 1.01±0.10 and 1.31±0.14 (Table 4). But, taking into account the 1 sigma error the two sets of ages agree in the case of samples Mgy1–2, Csm1–4 and Ft1–2, while

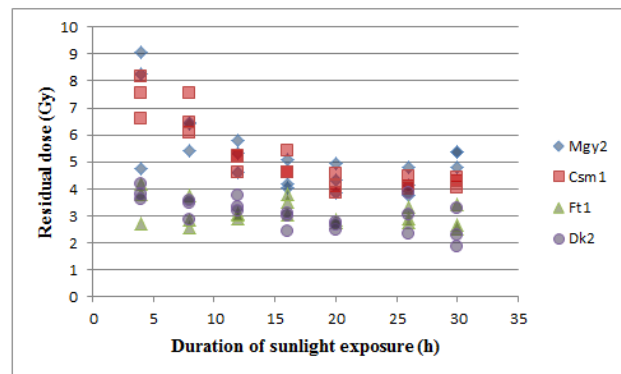


Fig 6. Change of post-IR IRSL₂₉₀ residual doses of four K-feldspar separates due to exposure to bright sunlight in summer. (The measured average natural doses are 100 Gy in Mgy2, 115 Gy in Csm1, 35 Gy in Ft1 and 36 Gy in Dk2.)

the K-feldspar ages of samples Dk1–5 agree within 2 sigma error limit with quartz ages.

Using the same post-IR IRSL₂₉₀ protocol on coarse-grain feldspar, there are some published data of residual doses, e.g. Alexanderson and Murray (2012) measured about 12 Gy residual dose in glaciofluvial sediments after 5 h bleaching in solar simulator in samples with 20–55 Gy natural dose; Thiel *et al.* (2012) and Buylaert *et al.* (2012) detected about 2 Gy and 5±2 Gy residuals in modern analogues of shallow marine and coastal sediments, respectively. Dating coarse-grain (0.16–0.25 mm) feldspar of coastal dune, Preusser *et al.* (2014) observed that prolonged (several days) daylight exposure leads to systematic, but only slightly lower residual D_e values. Ito *et al.* (2017) found unbleachable residual doses, and they subtracted it before age calculation. In their experiments, coarse-grain (0.18–0.25 mm) K-feldspar of beach sand was bleached under artificial sunlight up to 800 h, and the residual dose decreased from 15.7±1.8 Gy to 2.8±0.2 Gy. But, Colarossi *et al.* (2015) detected monotonic decrease of post-IR IRSL signals during 14 days exposure to artificial light in a solar simulator and did not find any unbleachable residual signal. In long-term (>80 days) laboratory bleaching experiments Yi *et al.* (2016) measured 6.2±0.7 Gy residual dose by post-IR IRSL₂₉₀. This residual dose was constant, or very difficult to bleach after ~300 h exposure to light in a solar simulator.

Some experiments, e.g. Buylaert *et al.* (2011), Li *et al.* (2013) and Preusser *et al.* (2014) proved that the residual dose increases with the increase of stimulation temperature, and presumably it mainly arises from thermal transfer effects due to preheat temperature (Buylaert *et al.* 2011).

Our bleaching experiment in bright sunlight in summer gave similar results (between 2.5±0.7 and 5.2±0.3 Gy residual doses after 30 h bleaching) to most of the above

mentioned earlier studies, among them, the outcomes of residual measurements of Thiel *et al.* (2012) and Buylaert *et al.* (2012) on modern sediments.

4.3 Quartz OSL and K-feldspar post-IR IRSL₂₉₀ ages of the dated sediments

In the southern part of the study area at Nagytarcsa, the fluvial gravelly sand layers of Danube terrace V, which contain saturated quartz and feldspar, are older than ~ 296 ka according to feldspar post-IR IRSL₂₉₀ minimum age based on $2 \cdot D_0$ values. Therefore, they were formed earlier than the MIS 7 period. This minimum age is not in conflict with the traditional terrace chronology of Pécsi (1959), Kretzoi and Pécsi (1982), and the 800 ka minimum age (Ruszkiczay-Rüdiger *et al.*, 2005a). The equivalent terrace in the Gerecse Hills developed between 2.4 and 1.0 Ma ago (Csillag *et al.*, 2018).

In the central part of the Pest Plain, the two aeolian fine sand layers on terrace V in the Mogyoród gravel mine are about 37–38 (± 3) ka old based on quartz ages (Table 4). In the case of the lower sample, the K-feldspar post-IR IRSL₂₉₀ age without the subtraction of any residual dose and the quartz OSL age are in excellent agreement and their ratio is 0.99 ± 0.10 . Consequently, after residual dose subtraction, the ratio between feldspar and quartz ages are 0.80 ± 0.08 and 0.92 ± 0.09 , depending on the bleaching conditions. In the upper sample, the age of feldspar without residual subtraction is older than the quartz age, while after the subtraction of the winter residual dose, it is younger than the quartz, the ratio of the feldspar age to quartz age is 1.10 ± 0.11 and 0.94 ± 0.10 , respectively (Table 4).

Here, the ages of the dune sand samples indicate wind activity in the cold and dry period of MIS 3 on the surface of terrace V. Aeolian sediments with similar ages were identified in other parts of Hungary, e.g. the ~39 ka old wind-blown sand in the southern part of Hungary at Katymár (Sümegei *et al.*, 2019, Fig. 1), the 41 ± 0.8 ka and 35 ± 5 ka old loess west from the study area at Süttö (Novothny *et al.*, 2010b), and 37–38 (± 3) ka old loess layers south from the study area at Paks (Thiel *et al.*, 2014; Fig. 1). In the other part of the Mogyoród gravel mine relict, sand-wedge polygons were studied as well earlier, and the infill sediments of a sand-wedge were 16–17 (± 2) ka old, dating with quartz OSL method (Fábián *et al.*, 2014).

In the northern part of the study area, on terrace III, the dated two aeolian silty fine sand samples in the East wall of the Csomád sand mine, deposited 43 ± 4 and 39 ± 3 ka ago in MIS 3, according to the quartz OSL ages. The post-IR IRSL₂₉₀ age of feldspar without residual-subtraction is similar to the age of quartz in the lower sample. In the case of the upper sample, the quartz age is between the age of feldspar without residual subtraction or with the subtraction of the summer residual dose after 4 h exposure to bright sunlight and the feldspar age after the subtraction of the winter

residual dose. The last one is the closest to the quartz age, their ratio is 0.96 ± 0.10 (Table 4).

The ages of the quartz in the fluvial sand samples in the West wall of this mine are 31 ± 3 and 29 ± 3 ka. The feldspar without residual subtraction gives older ages than the quartz with ratio 1.14 ± 0.12 (Csm4) and 1.09 ± 0.12 (Csm3). Meanwhile, after winter residual dose subtraction, the feldspar ages are younger, they are 0.94 ± 0.10 (Csm4) and 0.88 ± 0.10 (Csm3) of the quartz ages.

The ages of the dated samples in this mine indicate the formation of a sand dune in MIS 3, and fluvial sedimentation of a small stream about the transition from MIS 3 to MIS 2 on the surface of terrace III, which was formed minimum 170 ka ago (Ruszkiczay-Rüdiger *et al.*, 2005a). This 39–43 (± 4) ka old dune sand and the coeval loess in the area of Süttö and Paks (Novothny *et al.*, 2010b, Thiel *et al.*, 2014 respectively) prove strong wind activity in a cold and dry climate period of MIS 3. The fluvial sediments of a small stream at Csomád probably deposited during the warmer period at the end of MIS 3 or at the beginning of MIS 2 because chernozem-like soils formed about those times in the Katymár loess-paleosol sequence (Sümegei *et al.*, 2019).

In the Fót sand mine, also on the area of terrace III, the dated lower and upper sand layers of the slope sediments with reworked fluvial material, deposited during the MIS 2 period, 23 ± 2 and 15 ± 1 ka ago, based on quartz dating. The relation between the feldspar and quartz ages shows similar tendencies to most of the other dated samples. The feldspar ages without residual subtraction are older than the quartz ages with ratios 1.07 ± 0.10 and 1.05 ± 0.10 , while they are younger than the quartz after winter or summer residual subtraction, with ratios 0.83 ± 0.08 , 0.81 ± 0.08 and 0.94 ± 0.09 . The lower slope sediment was probably deposited during cold period, in the Last Glacial Maximum, because loess layers with similar ages were dated to the same periods at Katymár (~22.5 ka BP, Sümegei *et al.*, 2019) and Süttö (22 ± 2 ka, Novothny *et al.*, 2011).

On terrace IIb, in the Dunakeszi sand mine, fluvial sand layers of a stream were deposited about 15–16 (± 1) ka ago, and the age of the sand layers in a dune is about 14 ± 1 ka, according to quartz dating. Here is the largest difference between the feldspar ages which were calculated without residual dose subtraction and the quartz ages, the ratio of them ranges from 1.21 ± 0.12 to 1.31 ± 0.14 (Table 4). The feldspar ages after winter residual dose subtraction are younger than the quartz ages (feldspar age/quartz age is 0.87 ± 0.09 – 0.96 ± 0.10) except for the uppermost sample. Meanwhile, the feldspar of sample Dk2 after the subtraction of the summer residual dose gives an older age than the quartz does. The ages of the dated stream sediments and dune sands prove fluvial, and then aeolian activity during MIS 2 on the surface of terrace IIb, which developed a minimum 100 ka ago. In the southern part of

the study area, fluvial sand with a similar age (~16 ka) was dated by TL method at Dunavarsány (Fig. 2; Ujházi *et al.*, 2003; Gábris, 2003). 14 ka old dune sand was detected by the help of radiocarbon and luminescence dating in terrace IIa on the Szentendre Island at Kisoroszi (Fig. 2; Ujházi *et al.*, 2003; Gábris, 2003), in the Gödöllő Hills (Fig. 1) at Tura (Novothy *et al.* 2010a), and on other areas of Hungary as well, e.g. on the Nyírség alluvial fan (Fig. 1; Lóki *et al.*, 1994; Gábris, 2003; Buró *et al.*, 2014; Kiss *et al.*, 2015).

The 15-16(±1) ka old stream sediments of the Dunakeszi sand mine probably were deposited during the Oldest Dryas and the Allerød-Bølling interstadial, while the formation of the 14±1 ka old dune corresponds to the colder and drier period of the Allerød-Bølling according to the climate reconstruction of Kiss *et al.* (2015) with regards to Hungary.

Taking into account the differences between the ages of the dated two minerals, to get the same feldspar ages as the quartz ages, the assumable residual doses of the feldspar are set to be between 0 and 15±1 Gy (Csm1) or 0 and 24±2% (Dk1) of the measured natural doses (Table 4). These results imply that in most cases it is necessary to subtract some residual dose from the measured natural dose of feldspar before age calculation.

5. Conclusions

Optically stimulated luminescence dating of sandy fluvial, aeolian and slope sediments, collected on the Danube terraces of the Pest Plain serves new ages for this area where the numerical age data and the palaeontological findings are very scarce. Moreover it gives an opportunity for the comparison of coarse-grain quartz OSL and K-feldspar post-IR IRSL₂₉₀ ages of the same sediments.

The measured quartz medium aliquots show more heterogeneous dose distribution than the K-feldspar small aliquots. Probably, this is caused by the heterogeneity in the environmental beta dose rate and the internal alpha dose rate.

The feldspar post-IR IRSL₂₉₀ ages without residual dose subtraction are older than the quartz OSL ages, except for one sample, which quartz and feldspar ages are almost identical. But, the two sets of ages are overlapping within 1 or 2 sigma error.

References

- Adamiec G and Aitken M, 1998. Dose-rate conversion factors: update. *Ancient TL* 16(2): 37–50.
- Alexanderson H and Murray AS, 2012. Luminescence signals from modern sediments in a glaciated bay, NW Svalbard. *Quaternary Geochronology* 10: 250–256, DOI 10.1016/j.qua-geo.2012.01.001.
- Auclair M, Lamothe M and Huot S, 2003. Measurement of anomalous fading for feldspar IRSL using SAR. *Radiation Measurements* 37: 487–492, DOI 10.1016/s1350-4487(03)00018-0.
- Balescu S and Lamothe M, 1994. Comparison of TL and IRSL age estimates of feldspar coarse grains from waterlain

Our bleaching experiment showed that the residual dose of feldspar is from 2.5±0.7 Gy to 5.2±0.3 Gy or 3–8% of the measured natural dose after 30 h exposure to bright sunshine. Based on comparison with the quartz ages the assumable residual doses range from 0 Gy to 15±1 Gy and amount to 24±2% of the measured natural doses. Therefore, in most cases of our samples, some residual dose subtraction is necessary before the calculation of the post-IR IRSL₂₉₀ ages. However, without quartz OSL age data, or independent age control, the value of the residual dose of feldspar is uncertain. But, the range between the feldspar post-IR IRSL₂₉₀ age without residual-subtraction, and the residual-subtracted age, can be considered as the maximum age range of the sediment. For subtraction, the residual dose after 4 h exposure to light in a solar simulator or bright sunshine is favourable, because the post-IR IRSL₂₉₀ signal decreases rapidly in this time period.

The minimum age of the dated fluvial gravelly sand of terrace V is ~ 296 ka based on 2*D₀ values of feldspar post-IR IRSL₂₉₀. This age does not contradict the traditional terrace chronology and the earlier published age data of this terrace. The other studied sediments on the surface of the terraces V, III and IIb were deposited much later than the formation of the terraces. They indicate deposition of sediments in MIS 3 and MIS 2 periods: aeolian activity at 43–37(±3) ka and 14±1 ka ago, and fluvial sedimentation of small streams about 31–29(±3) ka and 16–15(±1) ka ago. The new ages help to reconstruct the surface developments of the Danube terraces. The age of the dated dune sands with coeval aeolian sediments in Hungary indicates the cold and dry periods with strong wind activity of the Late Weichselian.

Acknowledgements

A helpful introduction for Edit Thamó-Bozsó to post-IR-IRSL age dating by Dr. Sumiko Tsukamoto, Dr. Christine Thiel and Prof. Dr. Manfred Frechen at Leibniz Institute for Applied Geophysics (LIAG, Hannover) and help from Dr. Novothy Ágnes (Eötvös Loránd University, Budapest), Emese Thamó and Bálint Thamó are gratefully acknowledged. The comments of the reviewers significantly improved the final version of the paper, for which they are gratefully acknowledged. This research was supported by the Hungarian Scientific Research Fund (OTKA K 75801).

- sediments. *Quaternary Science Reviews* 13(5–7): 437–444, DOI 10.1016/0277-3791(94)90056-6.
- Borsy Z, 1989. Az Alföld hordalékkúpjainak negyedidőszaki fejlődéstörténete (Quaternary evolution of the alluvial fans of the Great Hungarian Plain). *Földrajzi Értesítő* 38(3–4): 211–224 (in Hungarian).
- Burján B, 2000. A Pesti-síkság fiatal kavicsos üledékeinek görgöttség-vizsgálata (Roundness examination of the young gravel sediments of Pest Plains). *Földrajzi Közlemények* 124(1–4): 61–74 (in Hungarian).
- Burján B, 2003. Budapest-környéki idős Duna-teraszok nehézsárvány-tartalmának statisztikai vizsgálata (Statistical investigations into heavy mineral composition of old Danubian terraces nearby Budapest, Hungary). *Földrajzi Értesítő* 52(3–4): 171–185 (in Hungarian).
- Buró B, Sipos Gy, Lóki J, András B, Félegyházi E and Négyesi G, 2014. Assessing late Pleistocene and Holocene phases of aeolian activity on the Nyírség alluvial fan, Hungary. *Quaternary International* 425: 183–195, DOI 10.1016/j.quaint.2016.01.007.
- Buylaert JP, Thiel C, Murray AS, Vandenberghe DAG, Yi S and Lu H, 2011. IRSL and post-IRSL residual doses recorded in modern dust samples from the Chinese loess plateau. *Geochronometria* 38: 432–440, DOI 10.2478/s13386-011-0047-0.
- Buylaert JP, Jain M, Murray AS, Thomsen KJ, Thiel C and Sobhati R, 2012. A robust feldspar luminescence dating method for Middle and Late Pleistocene sediments. *Boreas* 41: 435–451, DOI 10.1111/j.1502-3885.2012.00248.x.
- Colarossi D, Duller GTA, Roberts HM, Tooth S and Lyons R, 2015. Comparison of paired quartz OSL and feldspar post-IRSL dose distributions in poorly bleached fluvial sediments from South Africa. *Quaternary Geochronology* 30: 233–238, DOI 10.1016/j.quageo.2015.02.015.
- Csillag G, Fodor L, Kele S, Budai T, Kaiser M, Thamóné Bozsó E, Ruzsiczay-Rüdiger Zs, Sásdi L, Török Á, Lantos Z and Babinzski E, 2018. Pliocén–Kvarter (Pliocene–Quaternary). In: Budai T, ed., *A Gerecse hegység földtana: magyarázó a Gerecse hegység tájegységi földtani térképéhez (1:50000)*. *Geology of the Gerecse Mountains: Explanatory book to the geological map of the Gerecse Mountains (1:50000)*. Budapest, Magyar Bányászati és Földtani Szolgálat, 131–167 and 342–369 (In Hungarian and in English).
- Cunningham AC and Wallinga J, 2010. Selection of integration time intervals for quartz OSL decay curves. *Quaternary Geochronology* 5: 657–666, DOI 10.1016/j.quageo.2010.08.004.
- Dietze M, Kreutzer S, Burow C, Fuchs MC, Fischer M and Schmidt C, 2016. The abanico plot: visualising chronometric data with individual standard errors. *Quaternary Geochronology* 31: 12–18, DOI 10.1016/j.quageo.2015.09.003
- Fábián SÁ, Kovács J, Varga G, Sipos Gy, Horváth Z, Thamó-Bozsó E and Tóth G, 2014. Distribution of relict permafrost features in the Pannonian Basin, Hungary. *Boreas* 43: 722–732, DOI 10.1111/bor.12046.
- Fodor L, Bada G, Csillag G, Horváth E, Ruzsiczay-Rüdiger Zs, Palotás K, Síkhegyi F, Timár G, Cloetingh S and Horváth F, 2005. An outline of neotectonic structures and morphotectonics of the western and central Pannonian Basin. *Tectonophysics* 410: 15–41, DOI doi.org/10.1016/j.tecto.2005.06.008.
- Galbraith RF, 1988. Graphical display of estimates having differing standard errors. *Technometrics* 30: 271–281, DOI 10.1080/00401706.1988.10488400.
- Galbraith RF and Roberts RG, 2012. Statistical aspects of equivalent dose and error calculation and display in OSL dating: An overview and some recommendations. *Quaternary Geochronology* 11: 1–27, DOI 10.1016/j.quageo.2012.04.020.
- Galbraith RF, Roberts RG, Laslett GM, Yoshida H and Olley JM, 1999. Optical dating of single and multiple grains of quartz from Jinmium rock shelter, northern Australia: part I, experimental design and statistical models. *Archaeometry* 41: 339–364, DOI 10.1111/j.1475-4754.1999.tb00987.x.
- Gábris Gy, 1998. Late Glacial and Post Glacial development of drainage network and the paleohydrology in the Great Hungarian Plain. In: Bassa L and Kertész Á, eds., *Windows on Hungarian Geography*. Budapest, Akadémiai Kiadó: 23–36.
- Gábris Gy, 2002. A Tisza helyváltozásai (The shifting Tisza River). In: Mészáros R, Schweitzer F and Tóth J, eds., *Jakucs László, a tudós, az ismeretterjesztő és a művész*. Pécs, Magyar Tudományos Akadémia Földrajzi Kutatóintézet, Pécsi Tudományegyetem: 91–105 (in Hungarian).
- Gábris Gy, 2003. A földtörténet utolsó 30 ezer évének szakaszai és a futóhomok mozgásának főbb periódusai Magyarországon (The periods of the history of the Earth for the last 30 thousand years and the periods of the movement of aeolian sand). *Földrajzi Közlemények* 127(1–4): 1–14 (in Hungarian).
- Gábris Gy, 2006. A magyarországi folyóteraszok kialakulásának és korbeosztásának magyarázata az oxigénizotóp sztratigráfia tükrében (Formation and chronology of the Hungarian river terraces in the light of oxygen isotope stratigraphy). *Földrajzi Közlemények* 130(3–4): 123–133 (in Hungarian).
- Gábris Gy, 2013. A folyóvízi teraszok hazai kutatásának rövid áttekintése – a teraszok kialakulásának és korbeosztásának új magyarázata (Short review of the Hungarian investigations on fluvial terraces and new explication of the formation and time scale of the river terraces). *Földrajzi Közlemények* 137(3): 240–247 (in Hungarian).
- Gábris Gy and Nádor A, 2007. Long-term fluvial archives in Hungary: response of the Danube and Tisza rivers to tectonic movements and climatic changes during the Quaternary: a review and new synthesis. *Quaternary Science Reviews* 26: 2758–2782, DOI 10.1016/j.quascirev.2007.06.030.
- Gábris Gy, Horváth E, Novothny Á and Ruzsiczay-Rüdiger Zs, 2012. Fluvial and aeolian landscape evolution in Hungary – results of the last 20 years research. *Netherlands Journal of Geosciences* 91: 111–128, DOI 10.1017/s0016774600001530.

- Haas J, Budai T, Csontos L, Fodor L and Konrád Gy, 2010. *Magyarország pre-kainozoos földtani térképe, 1:500 000* (Pre-Cenozoic geological map of Hungary, 1:500 000). Budapest, Magyar Állami Földtani Intézet (in Hungarian and in English).
- Horváth F, 1993. Towards a mechanical model for the formation of the Pannonian basin. *Tectonophysics* 226: 333–357, DOI 10.1016/0040-1951(93)90126-5.
- Horváth F and Cloetingh S, 1996. Stress induced late-stage subsidence anomalies in the Pannonian Basin. In: Cloetingh S, Ben-Avraham Z, Sassi W and Horváth F, eds., Dynamics of extensional basins and inversion tectonics. *Tectonophysics* 266: 287–300, DOI 10.1016/s0040-1951(96)00194-1.
- Huntley DJ and Baril MR, 1997. The K content of the K-feldspars being measured in optical dating or in thermoluminescence dating. *Ancient TL* 15(1): 11–13.
- Ito K, Tamura T and Tsukamoto S, 2017. Post-IR IRSL dating of K-feldspar from last interglacial marine terrace deposits on the Kamikita coastal plain, northeastern Japan. *Geochronometria* 44: 352–365, DOI 10.1515/geochr-2015-0077.
- Jámbor Á, Moldvay L and Rónai A, 1966a. *Magyarország 200 000-es földtani térképsorozatához. Budapest, L-34-II.* (Explanatory book to the geological maps of Hungary 1:200 000). Budapest, Magyar Állami Földtani Intézet (in Hungarian).
- Jámbor Á, Moldvay L, Rónai A, Szentes F and Wein Gy, 1966b. *Magyarország földtani térképe 1:200 000* (Geological map of Hungary 1:200 000). Budapest, Magyar Állami Földtani Intézet (in Hungarian).
- Járáiné Komlódi M, 2000. A Kárpát-medence növényzetének kialakulása (Development of the vegetation of the Carpathian Basin). *Tilia* 9: 5–59 (in Hungarian).
- Kele S, 2009. *Édesvízi mészkövek vizsgálata a Kárpát-medencéből: paleoklimatológiai és szedimentológiai elemzések.* (Study of freshwater limestones from the Carpathian Basin: paleoclimatological and sedimentological implications). Budapest, PhD Thesis, Eötvös Loránd University: 176pp (in Hungarian).
- Kiss T, Hernesz P, Sümeghy B, Györgyövcics K and Sipos Gy, 2015. The evolution of the Great Hungarian Plain fluvial system – Fluvial processes in a subsiding area from the beginning of the Weichselian. *Quaternary International* 388: 142–155. DOI 10.1016/j.quaint.2014.05.050.
- Kretzoi M, 1981: Fontosabb szórványleletek a MÁFI Gerincesgyűjteményében (6. közlemény). (Wichtigere Streufunde in der Wirbeltiersammlung der Ungarischen Geologischen Anstalt, 6. Mitteilung). *Magyar Állami Földtani Intézet Évi Jelentése 1979-ről*: 483–490.
- Kretzoi M and Pécsi M, 1982. Pliocene and Quaternary chronostratigraphy and continental surface development of the Pannonian Basin. In: Pécsi M, ed., *Quaternary Studies in Hungary*. INQUA, MTA Földrajztudományi Kutató Intézet, Budapest: 11–42.
- Lantos M, 2004. Magnetostratigraphic correlation of Quaternary travertine sequences in NE Transdanubia. *Földtani Közlöny* 134(2): 227–236.
- Latham AG and Schwarcz HP, 1990. Magnetic polarity of travertine samples from Vértesszőlős. In: Kretzoi M and Dobosi TV, eds., *Vértesszőlős Site, Man and Culture*. Budapest, Akadémiai Kiadó: 553–555.
- Li B, Roberts RG and Jacobs Z, 2013. On the dose dependency of the bleachable and non-bleachable components of IRSL from K-feldspar: Improved procedures for luminescence dating of Quaternary sediments. *Quaternary Geochronology* 17: 1–13m DOI 10.1016/j.quageo.2013.03.006.
- Lóki J, Hertelendi E and Borsy Z, 1994. New dating of blown sand movement in the Nyírség. *Acta Geographica Ac Geologica et Meteorologica Debrecina* 32: 67–76.
- Magyar I, Radivojević D, Sztanó O, Synak R, Ujszászi K and Pócsik M, 2013. Progradation of the paleo-Danube shelf margin across the Pannonian Basin during the Late Miocene and Early Pliocene. *Global and Planetary Change* 103: 168–173, DOI 10.1016/j.gloplacha.2012.06.007.
- Mayya YS, Mortekai P, Murari MK and Singhvi AK, 2006. Towards quantifying beta microdosimetric effects in single-grain quartz dose distribution. *Radiation Measurements* 41: 1032–1039, DOI 10.1016/j.radmeas.2006.08.004.
- Mejdahl V, 1979. Thermoluminescence dating: beta-dose attenuation in quartz grains. *Archaeometry* 21(1): 61–72, DOI 10.1111/j.1475-4754.1979.tb00241.x.
- Mike K, 1991. *Magyarország ősvízrajza és felszíni vizeinek története* (The palaeoriver network of Hungary and the history of modern rivers). Budapest, AQUA kiadó: 698pp (in Hungarian).
- Murray AS, Schmidt ED, Stevens T, Buylaert JP, Marković SB, Tsukamoto S and Frechen M, 2014. Dating Middle Pleistocene loess from Stari Slankamen (Vojvodina, Serbia) – limitations imposed by the saturation behaviour of an elevated temperature IRSL signal. *Catena* 117: 34–42, DOI 10.1016/j.catena.2013.06.029.
- Neppel F, Somogyi S and Domokos M, 1999. A Duna és vízgyűjtőjének ősföldrajza (Palaeogeography of the Danube and its catchment). *Vízügyi Közlemények* 81(3): 499–514 (in Hungarian).
- Novothy Á, Barta G, Végh T, Bradák B, Surányi G and Horváth E, 2020. Correlation of drilling cores and the Paks brickyard key section at the area of Paks, Hungary. *Quaternary International* 552: 50–61, DOI 10.1016/j.quaint.2019.09.012.
- Novothy Á, Frechen M and Horváth E, 2010a. Luminescence dating of sand movement periods from the Gödöllő Hills, Hungary. *Geomorphology* 122: 254–263, DOI 10.1016/j.geomorph.2010.04.013.
- Novothy Á, Frechen M, Horváth E, Krbetschek M and Tsukamoto S, 2010b. Infrared stimulated luminescence and radiofluorescence dating of aeolian sediments from Hungary. *Quaternary Geochronology* 5(2-3): 114–119, DOI 10.1016/j.quageo.2009.05.002.
- Novothy Á, Frechen M, Horváth E, Wacha L and Rolf C, 2011. Investigating the penultimate and last glacial cycles of the Süttő loess section (Hungary) using luminescence dating,

- high-resolution grain size, and magnetic susceptibility data. *Quaternary International* 234(1–2): 75–85, DOI 10.1016/j.quaint.2010.08.002.
- Olley JM, De Deckker PD, Roberts RG, Fifield LK, Yoshida H and Hancock G, 2004. Optical dating of deep-sea sediments using single grains of quartz: a comparison with radiocarbon. *Sedimentary Geology* 169(3–4): 175–189, DOI 10.1016/j.sed-geo.2004.05.005.
- Pécsi M, 1958. A Pesti-síkság geomorfológiája (Geomorphology of the Pest Plain). In: Pécsi M, ed., *Budapest természeti képe* (Geography of Budapest). Budapest, Akadémiai Kiadó: 248–282 (in Hungarian).
- Pécsi M, 1959. *A magyarországi Duna-völgy kialakulása és felszínalakítása* (Formation and geomorphology of the Danube Valley in Hungary). Budapest, Akadémiai Kiadó: 346pp (in Hungarian).
- Pécsi M, 1996. *Geomorphological regions of Hungary*. Geographical Research Institute of the Hungarian Academy of Sciences, Budapest, 121pp.
- Pécsi M, Ádám L, Borsy Z, Buczkó E, Gazdag L, Góczán L, Hahn Gy, Kaiser M, Láng S, Leél-Őssy Sz, Lovász Gy, Marosi S, Pinczés Z, Rétvári L, Somogyi S, Székely A and Szilárd J, 2000. *Magyarország Geomorfológiai Térképe 1: 500 000* (Geomorphological map of Hungary 1: 500 000). MTA Földrajztudományi Kutató Intézet, Budapest.
- Pécsiné Donát É, 1958. Duna-terasz kavicsok görgetettségi vizsgálata (Investigations on the roundness of Danube terrace gravels). *Földtani Közlöny* 88(1): 57–75 (in Hungarian).
- Prescott JR and Hutton JT, 1994. Cosmic ray contribution to dose rates for luminescence and ESR dating: large depths and long-term time variations. *Radiation Measurements* 23(2–3): 497–500, DOI 10.1016/1350-4487(94)90086-8.
- Prescott JR and Stephan LG, 1982. The contribution of cosmic radiation to the environmental dose for thermoluminescent dating – Latitude, altitude and depth dependences. *PACT* 6: 17–25.
- Preusser F, Muru M and Rosentau A, 2014. Comparing different post-IR IRSL approaches for the dating of Holocene coastal foreshores from Ruhnu Island, Estonia. *Geochronometria* 41(4): 342–351, DOI 10.2478/s13386-013-0169-7.
- Rónai A, 1985. Az Alföld negyedidőszaki földtana. (The Quaternary of the Great Hungarian Plain). *Geologica Hungarica, series Geologica* 21: 446pp (in Hungarian).
- Ruszkiczay-Rüdiger Zs, Fodor L, Bada G, Leél-Őssy Sz, Horváth E and Dunai TJ, 2005a. Quantification of Quaternary vertical movements in the central Pannonian Basin: a review of chronologic data along the Danube River, Hungary. *Tectonophysics* 410(1–4): 157–172, DOI 10.1016/j.tecto.2005.05.048.
- Ruszkiczay-Rüdiger Zs, Dunai TJ, Bada G, Fodor L and Horváth E, 2005b. Middle to late Pleistocene uplift rate of the Hungarian Mountain Range at the Danube Bend (Pannonian Basin) using in situ produced ³He. *Tectonophysics* 410(1–4): 173–187, DOI 10.1016/j.tecto.2005.02.017.
- Ruszkiczay-Rüdiger Zs, Braucher R, Novothny Á, Csillag G, Fodor L, Madarász B and ASTER Team, 2016. Tectonic and climatic control on terrace formation: Coupling in situ produced 10Be depth profiles and luminescence approach, Danube River, Hungary, Central Europe. *Quaternary Science Reviews* 131: 127–147, DOI 10.1016/j.quascirev.2015.10.041.
- Ruszkiczay-Rüdiger Zs, Csillag G, Fodor L, Braucher R, Novothny Á, Thamó-Bozsó E, Virág A, Pazoni P, Tímár G and ASTER Team, 2018. Integration of new and revised chronological data to constrain the terrace evolution of the Danube River (Gerecse Hills, Pannonian Basin). *Quaternary Geochronology* 48: 148–170, DOI 10.1016/j.quageo.2018.08.003.
- Scheuer Gy and Schweitzer F, 1988. A Gerecse és a Budai-hegység édesvízi mészkőösszletei (Travertine sequences in the Gerecse and Buda Mountains). *Földrajzi Tanulmányok*: 20, Akadémiai Kiadó, Budapest, 120pp.
- Sierralta M, Kele S, Melcher F, Hambach U, Reinders J, Van Geldern R and Frechen M, 2010. Uranium-series dating of travertine from Süttő: implications for reconstruction of environmental change in Hungary. *Quaternary International* 222(1–2): 178–193, DOI 10.1016/j.quaint.2009.04.004.
- Somogyi S, 1961. Hazánk folyóhálózatának fejlődéstörténeti vázlata (Outline of the river network evolution of Hungary). *Földrajzi Közlöny* 85(1): 25–50 (in Hungarian).
- STD 2016: *Stratigraphische Tabelle von Deutschland 2016*. Deutsche Stratigraphische Kommission, Menning M and Hendrich A, eds., GeoForschungsZentrum Potsdam, http://www.stratigraphie.de/std/Bilder/5_2.pdf
- Sümegi P and Krolopp E, 1995. A magyarországi würm korú löszök képződésének paleoökológiai rekonstrukciója Mollusca-fauna alapján (Paleoecological reconstruction of Würmian loesses based on Mollusca fauna). *Földtani Közlöny* 125: 125–148 (in Hungarian).
- Sümegi P, Molnár D, Gulyás S, Náfrádi K, Sümegi BP, Töröcsik T, Persaits G, Molnár M, Vandenberghe J and Zhou L, 2019. High-resolution proxy record of the environmental response to climatic variations during transition MIS3/MIS2 and MIS2 in Central Europe: The loess-paleosol sequence of Katymár brickyard (Hungary). *Quaternary International* 504: 40–55, DOI 10.1016/j.quaint.2018.03.030.
- Szádeczky-Kardoss E, 1938. *Geologie der rumpfungarländischen Kleinen Tiefebene*. Sopron, 444pp (in German).
- Szádeczky-Kardoss E, 1941. Ősi folyók a Dunántúlon (Ancient rivers in Transdanubia). *Földrajzi Értésítő* 6(1): 119–134 (in Hungarian).
- Thiel C, Buylaert JP, Murray AS, Terhorst B, Hofer I, Tsukamoto S and Frechen M, 2011. Luminescence dating of the Stratzing loess profile (Austria) – Testing the potential of an elevated temperature post-IR IRSL protocol. *Quaternary International* 234(1–2): 23–31, DOI 10.1016/j.quaint.2010.05.018.
- Thiel C, Buylaert JP, Murray AS, Elmejdoub N and Jedoui Y, 2012. A comparison of TT-OSL and post-IR IRSL dating of coastal deposits on Cap Bon peninsula, north-eastern Tunisia. *Quaternary Geochronology* 10: 209–217, DOI 10.1016/j.quageo.2012.03.010.

- Thiel C, Horváth E and Frechen M, 2014. Revisiting the loess/palaeosol sequence in Paks, Hungary: A post-IR IRSL based chronology for the 'Young Loess Series'. *Quaternary International* 319: 88–98, DOI [10.1016/j.quaint.2013.05.045](https://doi.org/10.1016/j.quaint.2013.05.045).
- Ujházy K, Gábris Gy and Frechen M, 2003. Ages of periods of sand movement in Hungary determined through luminescence measurements. *Quaternary International* 111(1): 91–100, DOI [10.1016/S1040-6182\(03\)00017-X](https://doi.org/10.1016/S1040-6182(03)00017-X).
- Urbancsek J, 1960. Az alföldi artézi kutak fajlagos vízhozama és abból levonható vízföldtani és ősföldrajzi következtetések (Water productivity of the wells on the Great Hungarian Plain and its implications to hydrogeology and palaeogeography). *Hidrológiai Közöny* 40(5): 398–403.
- Virág A. 2013. *Magyarországi pliocén-pleisztocén elefanti-dae maradványok morfológiai és paleoökológiai vizsgálata* (Morphometrical and palaeoecological study of Hungarian Pliocene and Pleistocene Elephantids). Budapest, PhD Thesis, Eötvös Loránd University: 168pp (in Hungarian).
- Virág A and Gasparik M, 2012. Relative chronology of Late Pliocene and Early Pleistocene mammoth-bearing localities in Hungary. *Hantkeniana* 7: 27–36.
- Wintle A and Murray AS, 2006. A review of quartz optically stimulated luminescence characteristics and their relevance in single-aliquot regeneration dating protocols. *Radiation Measurements* 41(1): 369–391, DOI [10.1016/j.radmeas.2005.11.001](https://doi.org/10.1016/j.radmeas.2005.11.001).
- Yi S, Buylaert JP, Murray AS, Lu H, Thiel C and Zeng L, 2016. A detailed post-IR IRSL dating study of the Niuyangzigou loess site in northeastern China. *Boreas* 45(4): 644–657, DOI [10.1111/bor.12185](https://doi.org/10.1111/bor.12185).